

Plasmaspheric Helium Ion Distribution from Satellite Observations of HeII 304 Å

YAM T. CHIU
Space Sciences Laboratory
Laboratory Operations
The Aerospace Corporation
El Segundo, Calif. 90245

SUPRIYA CHAKRABARTI, FRANCESCO PARESCE,
and STUART BOWYER
Space Sciences Laboratory
University of California, Berkeley
Berkeley, Calif. 94720

ARTHUR AIKIN
NASA Goddard Space Flight Center
Greenbelt, Md. 20771

7 January 1982

APPROVED FOR PUBLIC RELEASE;
DISTRIBUTION UNLIMITED

LIBRARY COPY

JAN 5 1982

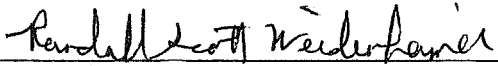
LANGLEY RESEARCH CENTER
LIBRARY, NASA
HAMPTON, VIRGINIA

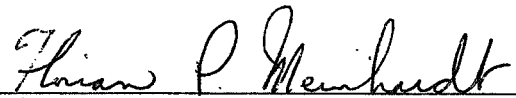
Prepared for
SPACE DIVISION
AIR FORCE SYSTEMS COMMAND
Los Angeles Air Force Station
P.O. Box 92960, Worldway Postal Center
Los Angeles, Calif. 90009

This report was submitted by The Aerospace Corporation, El Segundo, CA 90245, under Contract No.F04701-81-C-0082 with the Space Division, Deputy for Technology, P. O. Box 92960, Worldway Postal Center, Los Angeles, CA 90009. It was reviewed and approved for The Aerospace Corporation by G. A. Paulikas, Director, Space Sciences Laboratory. Lt Randall Weidenheimer, SD/YLVS, was the project officer for the Mission Oriented Investigation and Experimentation Program.

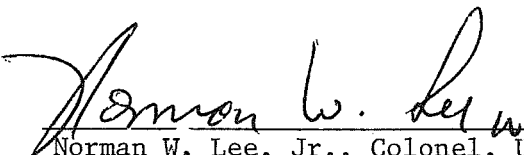
This report has been reviewed by the Public Affairs Office (PAS) and is releasable to the National Technical Information Service (NTIS). At NTIS, it will be available to the general public, including foreign nations.

This technical report has been reviewed and is approved for publication. Publication of this report does not constitute Air Force approval of the report's findings or conclusions. It is published only for the exchange and stimulation of ideas.


Randall S. Weidenheimer, Lt, USAF
Project Officer


Florian P. Meinhardt, Lt Col, USAF
Director of Advanced Space
Development

FOR THE COMMANDER


Norman W. Lee, Jr., Colonel, USAF
Deputy for Technology

UNCLASSIFIED

SECURITY CLASSIFICATION OF THIS PAGE (When Data Entered)

REPORT DOCUMENTATION PAGE		READ INSTRUCTIONS BEFORE COMPLETING FORM
1. REPORT NUMBER SD-TR-82-03	2. GOVT ACCESSION NO.	3. RECIPIENT'S CATALOG NUMBER
4. TITLE (and Subtitle) PLASMASPHERIC HELIUM ION DISTRIBUTION FROM SATELLITE OBSERVATIONS OF HeII 304Å		5. TYPE OF REPORT & PERIOD COVERED
		6. PERFORMING ORG. REPORT NUMBER TR-0082(2940-04)-1
7. AUTHOR(s) Y. T. Chiu, S. Chakrabarti, F. Paresce, S. Bowyer and A. Aikin		8. CONTRACT OR GRANT NUMBER(s) F04701-81-C-0082
9. PERFORMING ORGANIZATION NAME AND ADDRESS The Aerospace Corporation El Segundo, Calif. 90245		10. PROGRAM ELEMENT, PROJECT, TASK AREA & WORK UNIT NUMBERS
11. CONTROLLING OFFICE NAME AND ADDRESS Space Division Air Force Systems Command Los Angeles, Calif. 90009		12. REPORT DATE 7 January 1982
		13. NUMBER OF PAGES 18
14. MONITORING AGENCY NAME & ADDRESS (if different from Controlling Office)		15. SECURITY CLASS. (of this report) Unclassified
		15a. DECLASSIFICATION/DOWNGRADING SCHEDULE
16. DISTRIBUTION STATEMENT (of this Report) Approved for public release; distribution unlimited		
17. DISTRIBUTION STATEMENT (of the abstract entered in Block 20, if different from Report)		
18. SUPPLEMENTARY NOTES		
19. KEY WORDS (Continue on reverse side if necessary and identify by block number) Density Model Extreme Ultraviolet Emission Helium Plasmasphere		
20. ABSTRACT (Continue on reverse side if necessary and identify by block number) High sensitivity and spatial resolution observations of the HeII-304 Å emission line intensity in the earth's nightglow have been carried out by the extreme ultraviolet telescope on the Apollo-Soyuz mission in July 1975. The data, obtained over a wide range of plasmasphere parameters, are compared with the predictions of a kinetic equilibrium model of plasmaspheric ion density. Excellent overall agreement between observation and theory is found using as inputs a temperature model, solar flux, and H ⁺ and O ⁺ number densities		

19. KEY WORDS (Continued)

20. ABSTRACT (Continued)

determined by extrapolating nearly simultaneous Atmospheric Explorer C measurements at 300 km. The observations in the northern hemisphere are well fit by a model having $285 \text{ He}^+ \text{ ions cm}^{-3}$ at 500 km independent of latitude or longitude while those in the south require $430 \text{ He}^+ \text{ ions cm}^{-3}$ at the same altitude. This result is consistent with available information on the interhemispheric asymmetry of He^+ observed by a mass spectrometer on Explorer 32 and on the winter neutral helium bulge.

Acknowledgments

We thank Drs. Michael Lampton, Bruce Margon, Robert Stern, and Jay Freeman for their assistance with instrument testing, integration and ground operations during the ASTP flight.

This work was also supported by NASA grant NGR05-003-450 and NAG5-139. One author, Supriya Chakrabarti, acknowledges the support of a Centenary Scholarship from the Bengal Chamber of Commerce and Industry.

CONTENTS

ACKNOWLEDGMENTS.....	1
I. INTRODUCTION.....	7
II. OBSERVATIONS.....	8
III. ANALYSIS AND DISCUSSION.....	11
SUMMARY AND CONCLUSIONS.....	17
REFERENCES.....	19

FIGURES

1. Intensity of the observed 304 Å feature in Rayleighs plotted as a function of UT shown with crosses..... 10
2. The schematic of the viewing geometry in the noon-midnight plane..... 12

I. Introduction

Measurement of the intensity and spatial variations of the resonantly scattered HeII-304 Å emission line in the earth's airglow represents an important and perhaps unique method for determining the global distribution of thermal He^+ in the plasmasphere (Young et al. 1971a). For this reason, a number of such measurements have been carried out (Young et al. 1971b; Ogawa and Tohmatsu, 1971; Meier and Weller, 1972; Paresce et al., 1973, 1974; Weller and Meier, 1974), and a number of theoretical calculations performed (Schunk and Walker, 1970; Murphy et al., 1979; Chiu et al., 1979; Raitt et al., 1978; Ottley and Schunk, 1980 and the references therein). Due to the low sensitivity (a few counts $\text{s}^{-1} \text{Rayleigh}^{-1}$) and low spatial resolutions ($\approx 10^\circ$ FWHM) of these observations, simple ad-hoc models of the plasmaspheric He^+ distributions such as constant density, power law or diffusive equilibrium models, have been found to fit the available data reasonably well and have been useful in deriving results whose accuracy is comparable to the large uncertainties in the models and the data. The EUV telescope on the Apollo-Soyuz mission (ASTP) has carried out a comprehensive study of the HeII-304 Å nightglow with orders of magnitude more sensitivity (860 counts $\text{s}^{-1} \text{Rayleigh}^{-1}$) and much higher spatial resolution (2.5° FWHM) than heretofore available. Results of a preliminary analysis of these data using the models just described have been reported by Chakrabarti et al. (1980). These authors showed that these models were inadequate to explain the complex variations of the observed signal obtained over such a wide range of plasmasphere parameters and were thus of limited usefulness in obtaining an accurate and realistic determination of the He^+ distribution. In this report, the results of a comparison of the ASTP HeII-304 Å observations with the predictions of a self-consistent kinetic equilibrium model of the

plasmaspheric ion density described by Chiu et al. (1979) are given, and the implications of such a comparison on our understanding of the global distribution of thermal plasma in the earth's atmosphere are discussed.

II. Observations

The data discussed here were acquired by the extreme ultraviolet telescope (EUVT) carried into a 215 km altitude earth orbit by the Apollo-Soyuz mission (ASTP) in July 1975. The telescope (described in more detail in Lampton et al., 1976; and Bowyer et al., 1977) consists of a 37 cm diameter grazing incidence flux collector, a continuously rotating six position filter wheel and a pair of channel electron multiplier photon detectors. The experiment was operated as a five color photometer with the combination of thin film filters and the response of the detector and optics defining bandpasses of 45-185, 114-185, 170-620, 500-780, and 1350-1700 Å. An opaque position on the filter wheel permits nearly continuous monitoring of inherent detector background during the observations.

Count rates from both detectors are telemetered each 0.1 sec, cyclically providing 0.7 seconds accumulation of data at each bandpass every six seconds. The field of view of the instrument is circular with a sharply defined trapezoid profile with selectable widths of 2.5 and 4.3° FWHM obtained by commanding either of the detectors into the focal position. The instrument sensitivity as a function of wavelength for the bandpasses relevant to our discussion in this report is given by Paresce et al., 1981.

The 170-620 Å bandpass defined by an aluminum and carbon thin film filter has a non-negligible residual sensitivity at the wavelength of the resonance line of neutral helium at 584 Å, also a prominent feature of the night sky in the EUV. Its intensity can be measured with the 500-780 Å EUVT

passband defined by the tin thin film filter and its contribution to the signal in the 170-620 Å band assessed and removed to yield the 304 Å intensity alone. For a typical intensity of the 584 Å line of 1 Rayleigh (Freeman et al., 1977), the sensitivity of the instrument to 304 Å radiation is $860 \text{ counts s}^{-1} \text{ Rayleigh}^{-1}$ for the 2.5° FWHM detector.

The experiment was operated primarily in a pointed mode using the Apollo guidance system to orient the spacecraft and the telescope at a number of pre-selected stellar target. As the telescope was slewed from one target to the other and as the spacecraft moved from north to south in its 55° inclination orbit, a large region of the night sky was covered by the instrument. A typical scan of the night sky obtained in this way with the 2.5° FWHM detector is shown in figure 1. The observed intensity in Rayleighs ($1 \text{ Rayleigh} = 10^6/4\pi \text{ photons sec}^{-1} \text{ cm}^{-2} \text{ sr}^{-1}$) of 304 Å radiation during the maneuvers as a function of UT in seconds after 1200 UT July 21, 1975 appears in the upper panel of this figure (crosses).

The observations were made at local spacecraft times between 1900 and 0500 hours. The first part of this pass between UT \approx 2300 seconds and 2800 seconds, covered the northern latitudes of the plasmasphere, while between UT \approx 3200 and \approx 3800, the line of sight was completely contained in the earth's shadow. Finally, the southern hemisphere was explored at UT $>$ 2800 seconds. The model predictions, discussed in detail in section III, are shown with full lines in figure 1. The lower panel displays the corresponding values of the distance R in Earth radii from the Earth's center at which the line of sight breaks into sunlight. We define this point to be P_1 . Also shown are the invariant magnetic latitudes of the point P_1 for the corresponding lines of sight. The magnetic latitude and longitudes of the spacecraft ranged from 19.4° and 14.0° E at T = 2300 to

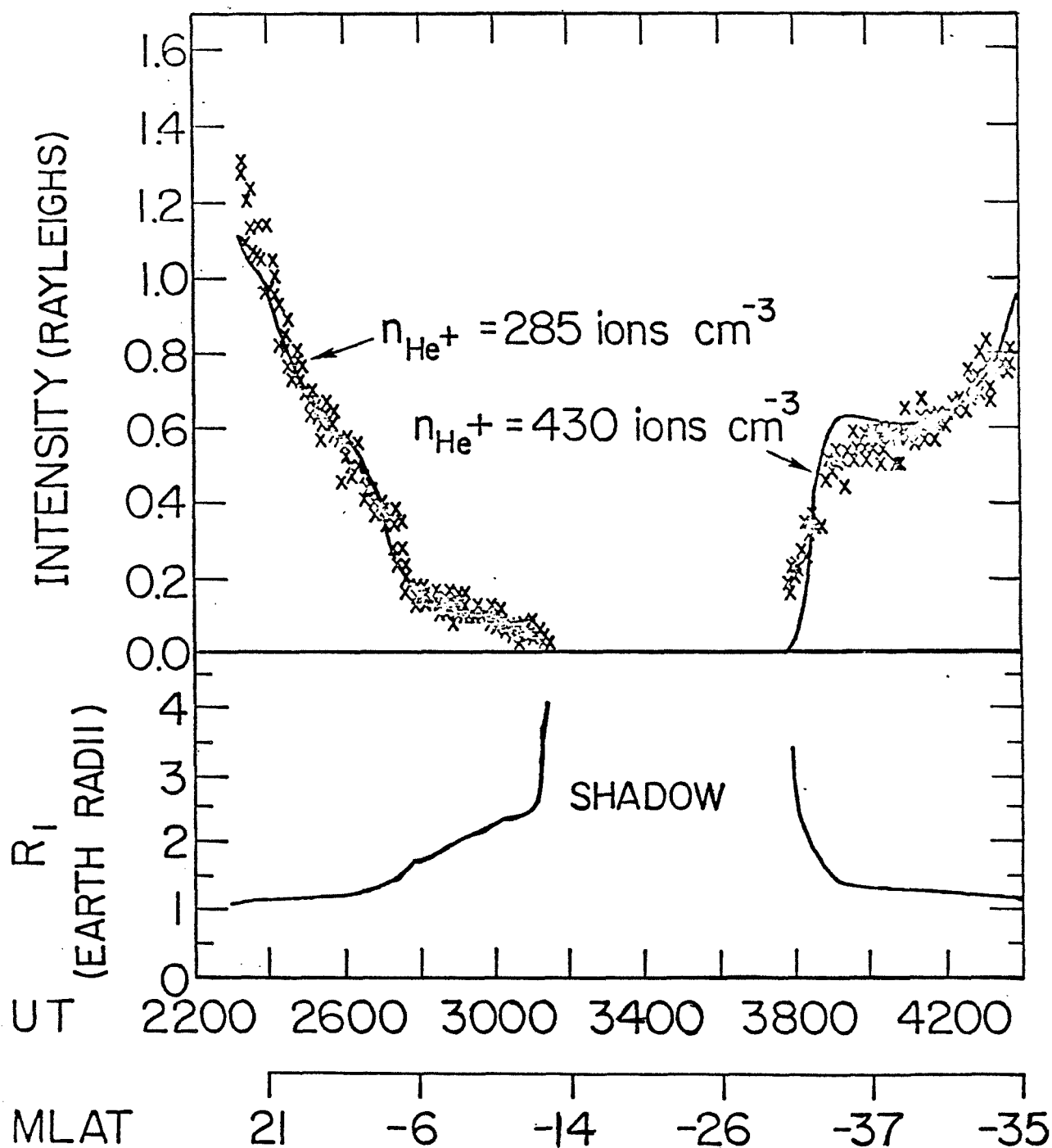


Figure 1. Intensity of the observed 304 Å feature in Rayleighs plotted as a function of UT shown with crosses. The model predictions are shown with the solid line. The altitude (R_1) of the point (P_1) (see figure 2) where the line of sight breaks into sunlight is shown in the bottom panel for the corresponding points. Also shown is the magnetic latitude of P_1 for the corresponding times.

-40.9° and -31.5° W at T = 4400 seconds respectively. The appropriate viewing geometry is shown in figure 2. The shadow height was taken to lie at 300 km. where the transmission of the 304 Å feature through the atmosphere is 10% (Paresce et al. 1973).

III. Analysis and Discussion

The expected intensity of the 304 Å radiation in Rayleighs in a scattering medium which is isothermal, optically thin and at rest with respect to the earth can be shown (Paresce et al. 1973) to be given by:

$$I = 10^{-6} A \int_z p(\theta) (\pi F_{\nu})_0 f \left(\frac{\pi e^2}{m_e c} \right) n(\text{He}^+) dz \quad (1)$$

where z is the line of sight direction, $p(\theta)$ is the phase function for scattering through an angle θ , $(\pi F_{\nu})_0$ is the solar flux at the line center, f is the oscillator strength of the 304 Å transition, $n(\text{He}^+)$ is the number density of He^+ in the plasmasphere, A is the attenuation factor for pure absorption at 304 Å by thermospheric N_2 , O_2 and O . This factor is calculated for the conditions appropriate to the time of flight using the MSIS model using data from mass spectrometers on five satellites and four ground-based incoherent scatter stations (Hedin, 1979). The scattering phase function $p(\theta)$ for 304 Å is (Brandt and Chamberlain, 1959)

$$P(\theta) = 1 + 1/4 (2/3 - \sin^2 \theta) \quad (2)$$

where θ is the angle between the line of sight and the sun-scatterer direction. The value of the integrated solar line flux at 304 Å used in

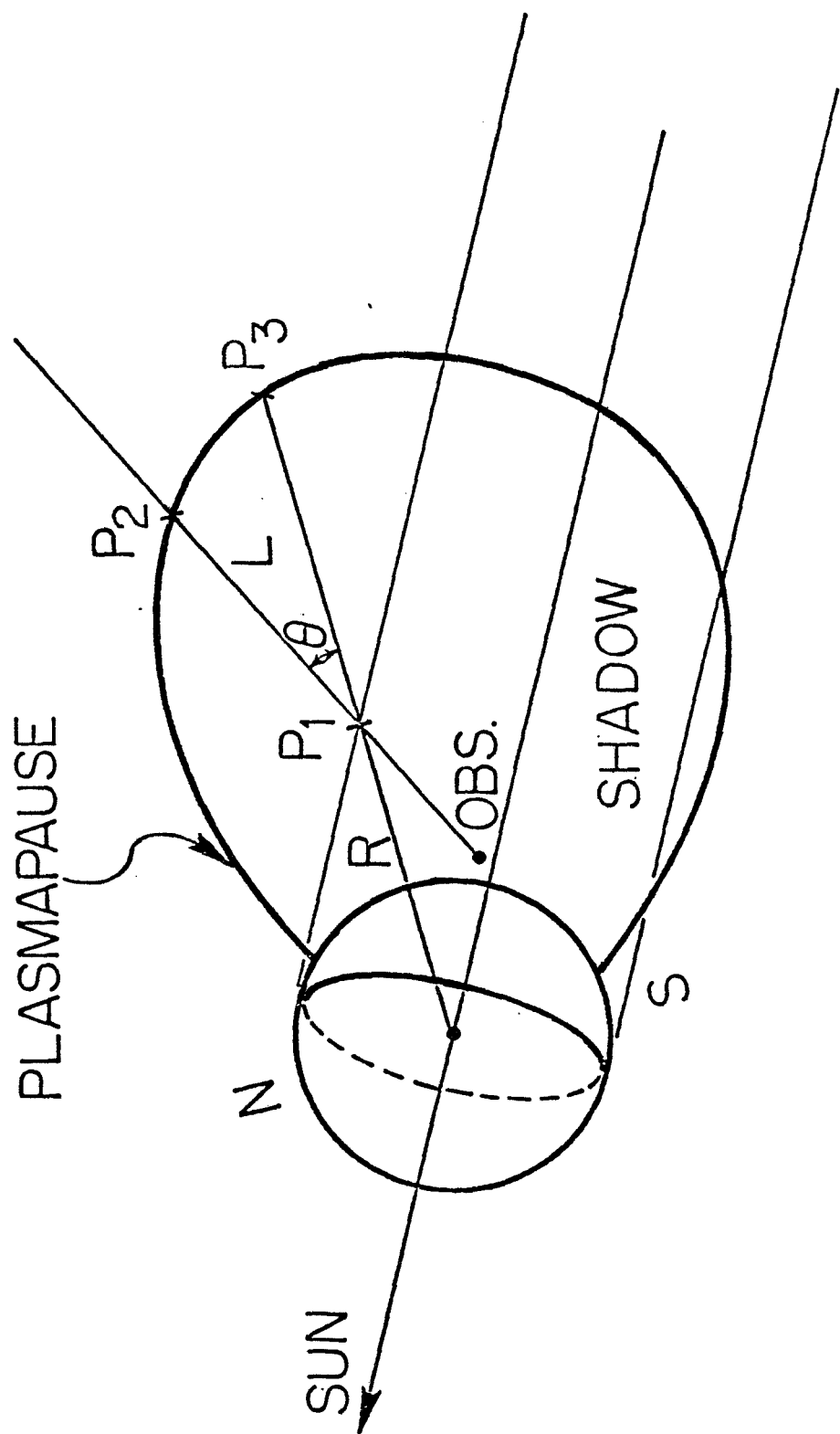


Figure 2. The schematic of the viewing geometry in the noon-midnight plane.

our calculation was 7.1×10^9 photons cm^{-2} sec^{-1} . This value was obtained by the EUV spectrometer on the AE-E satellite during the solar quiet period of July 13-28, 1976 ($\bar{F} = 67$) (Hinteregger et al. 1981) in the 300-350 Å passband. This value is consistent with observations by Heroux and Higgins (1977), whose measured solar flux at HeII-304 Å was 6.9×10^9 and 7.4×10^9 photons cm^{-2} sec^{-1} under similar solar conditions ($\bar{F} = 74$ and 84 respectively) in 1973. Using 0.15 Å as the width of the solar 304 Å line (Behring et al. 1972), eq. (1) reduces to

$$I = 1.05 \times 10^{-11} A P(\theta) \int_z n(\text{He}^+) dz . \quad (3)$$

Thus, the observed intensity essentially depends upon the integrated column density of the He^+ ions along the line of sight. This is computed by integrating the model's predicted number density profile from the lower to the upper bound of the illuminated column (points P_1 and P_2 respectively in figure 2). The latter is derived from the standard statistical relationship between the plasmaspheric radius and the interplanetary K_p index at the time of observation (Binsack, 1967; Carpenter and Park, 1973).

The He^+ ion distribution we adopted is based on a model discussed in detail by Chiu et al., 1979. The model has features similar to the conventional diffusive equilibrium distribution of collisionless plasmas (see, for example, Bauer 1969) with the important difference of the inclusion of an inhomogeneous magnetic force in the force balance equation. This force, required by kinetic considerations, is significant for the case of low and medium density plasmas, and thus is important in the plasmasphere. In this model, the distribution of He^+ ions of masses m_{He^+} at a radial distance r from the center of the earth is given by

$$n(\text{He}^+) = n_{\text{He}^+}^{(\ell)} \left[\frac{B_s}{B_\ell} \cdot \frac{T(\ell)}{T(s)} \right] \exp \left\{ \int_\ell^S \left[eE - m_{\text{He}^+} \left(\frac{GM_E}{r^2} + \Omega_E^2 r \right) \hat{r} \cdot \hat{s} \right] / kT(s) ds \right\} \quad (4)$$

where s is the arc length along a dipolar flux tube defined to be zero at the equator and $s = \ell$ at the reference altitude (500 km), $n_{\text{He}^+}^{(\ell)}$ is the He^+ number density at $s = \ell$ and $T(s)$ is the temperature structure of the plasmasphere, G is the gravitational constant, M_E is the earth's mass, and Ω_E is the earth's angular speed. The ion distribution depends upon the magnetic field B_s at s and the self-consistent ambipolar diffusion electric field, E . The plasmasphere is assumed to consist of only three kinds of ions: O^+ , H^+ , and He^+ . The equilibrium solution is obtained by requiring charge neutrality, i.e.

$$n_e(s) = n_{\text{O}^+}(s) + n_{\text{H}^+}(s) + n_{\text{He}^+}(s) \quad (5)$$

The model is completely specified once the temperature structure $T(s)$ and the ionospheric density n_{He^+} at the reference altitude are specified. As suggested by Chiu et al., the temperature profile was modelled by

$$T(s) = T_0 C F_{LT}(t) + T_1 \left(\frac{L-1}{L_0} \right)^\alpha \left(\frac{\ell-s}{\ell} \right)^\beta \quad (6)$$

where α determines the temperature variation as a function of L and β determines the variation of temperature as a function of s along a field line for a given L . T_0 is the ion temperature measured by the Retarding Potential

Analyzer on board the AE-C satellite at 300 km at 0600 hours local time near the magnetic equator during the time of our observation. C is a scale factor which scales the AE-C observations to yield temperatures at 500 km altitude at the foot of the field lines along the line of sight. This was obtained from a standard temperature-altitude model (Banks and Kockarts, 1973). $F_{LT}(t)$ is a factor which accounts for the variations of temperature with local time (t) and is determined from AE-C measured temperatures in the same local time zones as ours about a week before and a week after our observations under identical solar and geomagnetic conditions. The function $F_{LT}(t)$ has approximately the shape of a sine wave which gives a temperature of 800° K at 00 hours and 2000° K at 0600 and 1800 hours.

The values of the different parameters used in modelling the temperature structure are as follows:

$$T_0 = 2000^\circ \text{ K}, S = 1.21, T_1 = 7000^\circ \text{ K}, \alpha = \beta = 0.5, L_0 = 2$$

These parameters yield a temperature of about $11,000^\circ \text{ K}$ at the equatorial plasmopause consistent with the available measurements discussed in detail in Chiu et al. 1979. In this analysis, we have assumed that the number density of H^+ and O^+ ions at 500 Km do not vary with latitude, local time, etc. inside the plasmasphere. The number densities of H^+ and O^+ at the boundary ionosphere used in this analysis were obtained by the Bennett ion mass spectrometer on board the AE-C satellite at 300 Km at the time of our flight. We extrapolated these values to 500 Km using an ionosphere model incorporating flow along magnetic flux tubes as well as production and loss of ionization (Young et al. 1980). The number densities O^+ and H^+ at the reference altitude (500 Km) appropriate for our conditions were found to be 40,000 and 1,000 ions cm^{-3} respectively.

We have used the He^+ number density at 500 km as the free parameter. Unlike the O^+ , H^+ densities, we have allowed for a north-south asymmetry in the He^+ distribution at 500 Km. We have included a winter He^+ bulge at 500 Km, such as that possibly observed by Brinton et al. 1969, by using two different number densities in the two hemispheres. Since He^+ is produced by photoionization of neutral helium, this winter He^+ bulge could be associated with the observed neutral helium bulge (Keating and Prior, 1968)

In order to study the sensitivity of the model predictions to the input O^+ , H^+ number densities and the temperature (T_0) at 500 Km we varied them and found the following:

1. A factor of two change in the O^+ and H^+ densities change the theoretical HeII 304 Å intensity by about 8 percent each. So a realistic variation of O^+ and H^+ densities with latitude at 500 Km, will have a minimal effect on the calculated intensities and will be well within the uncertainties in the measurement.
2. The model is more sensitive to T_0 than O^+ or H^+ densities. A factor of two change in T_0 changes the predicted intensity of the 304 Å feature by ~ 30 percent. The plasma temperature variation with latitude at 400 Km between 60°N and 60°S was found to be $\sim 30\%$ (Titheridge 1976). Such a variation will change the model's prediction by $\sim 10\%$ and will be within the absolute accuracy of the measurement.

The overall best fit was obtained with a model having a He^+ number density of 285 cm^{-3} at 500 Km in the north (summer) hemisphere and 430 ions cm^{-3} in the southern hemisphere shown as a solid line in figure 1. The excellent overall fit to our observations with the model predictions

using AE data at the time of flight as boundary values confirm the basic validity of the Chiu et al. model. It also shows that HeII-304 Å photometry can be unfolded to yield plasmaspheric ion distributions. The temperature structure and the boundary ionospheric number densities are the only input parameters to the model. Since the input ionospheric model did not include any variations with latitude, local time, etc., the good agreement of model predictions and observations indicates that the overall features in the observations are primarily controlled by the plasmaspheric temperature structure and the ion density at 500 Km. Moreover, this also implies that our assumed temperature distribution should be a good representation of the actual one.

Summary and Conclusions

We have presented the first derivation of the plasmaspheric He^+ ion distribution employing satellite measurements of scattered HeII-304 Å resonance radiation observed by the extreme ultraviolet telescope on the Apollo-Soyuz mission. Emission can be explained by a He^+ distribution computed with the aid of a plasmaspheric model. Magnetic field inhomogeneities as well as collisions, and temperature changes within the plasmasphere are included. Normalization to ion densities, temperatures and composition observed simultaneously near the altitude of the lower boundary enhances the effectiveness of the model. The derived He^+ distribution has a midlatitude summer to winter ratio of 0.6 at 500 km. This ratio is consistent with seasonal changes in neutral helium at 500 Km which influences the photoionization rate. The loss of He^+ by charge exchange to O_2 and N_2 will also be less in winter at 500 km leading to further the enhancement of He^+ .

Satellite observations of extreme ultraviolet emissions from H^+ , O^+ , and He^+ affords an excellent opportunity to explore remotely the plasmaphere and ionosphere. In the present instance the plasmaspheric He^+ distribution from 500 to 30,000 Km has been determined.

References

- Banks, P.M. and G. Kockarts, Aeronomy, Part B, Academic, New York, 1973.
- Bauer, S.J., Diffusive Equilibrium in the Topside Ionosphere, Proc. IEEE, 57, 1114, 1969.
- Behring, W.E., L. Cohen, and U. Feldman. The Solar Spectrum: Wavelengths and Identification from 60-385 Å, Astrophys. J., 175, 493, 1972.
- Binsack, H.H., Plasmopause Observations with the MIT Experiment on Imp 2, J. Geophys. Res., 72, 5321, 1967.
- Bowyer, S., B. Margon, M. Lampton, F. Paresce, and R. Stern, Extreme Ultraviolet Survey Experiment MA-083, ASTP Summary Science Report, NASA SP-412, 1, 49, 1977.
- Brandt, J.C., and J.W. Chamberlain, Interplanetary Gas, 1, Hydrogen Radiation in the Night Sky, Astrophys. J., 130, 670, 1959.
- Brinton, H.C., R.A. Pickett, and H.A. Taylor, Diurnal and Seasonal Variations of Atmospheric Ion Compositions; Correlation with Solar Zenith Angle, J. Geophys. Res., 74, 4064, 1969.
- Carpenter, D.L. and C.G. Park, On What Ionospheric Workers Should Know About the Plasmopause-Plasmasphere, Rev. Geophys. Space Phys., 11, 133, 1973.
- Chakrabarti, S., F. Paresce, and S. Bowyer, The Distribution of Single Ionized Ionospheric Helium from 304 Å Backscatter Observations. Space Research, XX, edited by M.S. Rycroft, PL&L, Pergamon, Oxford and New York, 1980.
- Chiu, Y.T., J.G. Luhmann, B.K. Ching, and D.J. Boucher, Jr., An Equilibrium Model of Plasmaspheric Composition and Density, J. Geophys. Res., 84, 909, 1979.

- Freeman, J., F. Paresce, S. Bowyer, M. Lampton, R. Stern, B. Margon, The Local Interstellar Helium Density, Astrophys. J. (Letters), 215, L83, 1977.
- Hedin, A.E., Tables of Thermospheric Temperature, Density and Composition Derived from Satellite and Ground Based Measurements, Vol. 1, Ap = 4, Goddard Space Flight Center, January, 1979.
- Heroux, L. and J.E. Higgins, Summary of Full-Disk Solar Fluxes Between 250 and 1940 Å, J. Geophys. Res., 82, 3307, 1977.
- Hinteregger, H.E., H. Fukui, and B.R. Gilson, Solar EUV AE-E Satellite Observations and Aeronomical Model Representation for Cycle 21, in press, 1981.
- Keating, G. and E.J. Prior, The Winter Helium Bulge, Space Research 8, 982, 1968.
- Lampton, M., B. Margon, F. Paresce, R. Stern, and S. Bowyer, Discovery of a Non-Solar Extreme Ultraviolet Source, Astrophys. J. (Letters), 203, L71, 1976.
- Meier, R.R., and C.S. Weller, EUV Resonance Radiation from Helium Atoms and Ions in the Geocorona, J. Geophys. Res., 77, 1190, 1972.
- Murphy, J.A., G.J. Bailey, and R.J. Moffett, Helium Ions in the Mid-Latitude Plasmasphere, Planet. Space Sci., 27, 1441, 1979.
- Ogawa, T., and T. Tohmatsu, Sounding Rocket Observation of Helium 304 Å and 584 Å Glow, J. Geophys. Res., 76, 6136, 1971.
- Ottley, J.A. and R.W. Schunk, Density and Temperature Structure of Helium Ions in the Topside Polar Ionosphere for Subsonic Outflows, J. Geophys. Res., 85, 4177, 1980.
- Paresce, F., S. Bowyer and S. Kumar, Observations of the HeII 304 Å Radiation in the Night Sky, J. Geophys. Res., 78, 71, 1973.

- Paresce, F., S. Bowyer, and S. Kumar, On the Distribution of the He^+ in the Plasmasphere from Observations of Resonantly Scattered HeII 304 Å Radiation, J. Geophys. Res., 79, 174, 1974.
- Paresce, F., H. Fahr, and G. Lay, A Search for Interplanetary HeII 304 Å Radiation, J. Geophys. Res., in press, 1981.
- Raitt, W.J., R.W. Schunk, and P.M. Banks, Quantitative Calculations of Helium Ion Outflow from the Terrestrial Ionosphere, Planet. Space Sci., 26, 255, 1978.
- Schunk, R.W. and J.C.G. Walker, Thermal Diffusion in the Topside Ionosphere for Mixtures which Include Multiply-Charged Ions, Planet. Space Sci., 17, 853, 1969.
- Titheridge, J.E., Plasma Temperatures from Alouette 1 Electron Density Profiles, Planet. Space Sci., 24, 247, 1976.
- Weller, C.S. and R.R. Meier, First Satellite Observations of the He^+ 304 Å Radiation and its Interpretation, J. Geophys. Res., 79, 1572, 1974.
- Young, E.R., P.G. Richards, and D.G. Torr, A Flux Preserving Method of Coupling First and Second Order Equations to Simulate the Flow of Plasma Between the Photosphere and the Ionosphere, J. of Comput. Physics, 38, 141, 1980.
- Young, J., G.R. Carruthers, J.C. Holmes, C.Y. Johnson, and N.P. Patterson, Detection of Lyman β and Helium Resonance Radiation in the Night Sky, Science, 160, 990, 1971a.
- Young, J.M., C.S. Weller, C.Y. Johnson, and J.C. Holmes, Rocket Observations of the Far UV Nightglow at Lyman α and Shorter Wavelengths, J. Geophys. Res., 76, 3710, 1971b.

LABORATORY OPERATIONS

The Laboratory Operations of The Aerospace Corporation is conducting experimental and theoretical investigations necessary for the evaluation and application of scientific advances to new military space systems. Versatility and flexibility have been developed to a high degree by the laboratory personnel in dealing with the many problems encountered in the nation's rapidly developing space systems. Expertise in the latest scientific developments is vital to the accomplishment of tasks related to these problems. The laboratories that contribute to this research are:

Aerophysics Laboratory: Launch vehicle and reentry aerodynamics and heat transfer, propulsion chemistry and fluid mechanics, structural mechanics, flight dynamics; high-temperature thermomechanics, gas kinetics and radiation; research in environmental chemistry and contamination; cw and pulsed chemical laser development including chemical kinetics, spectroscopy, optical resonators and beam pointing, atmospheric propagation, laser effects and countermeasures.

Chemistry and Physics Laboratory: Atmospheric chemical reactions, atmospheric optics, light scattering, state-specific chemical reactions and radiation transport in rocket plumes, applied laser spectroscopy, laser chemistry, battery electrochemistry, space vacuum and radiation effects on materials, lubrication and surface phenomena, thermionic emission, photosensitive materials and detectors, atomic frequency standards, and bioenvironmental research and monitoring.

Electronics Research Laboratory: Microelectronics, GaAs low-noise and power devices, semiconductor lasers, electromagnetic and optical propagation phenomena, quantum electronics, laser communications, lidar, and electro-optics; communication sciences, applied electronics, semiconductor crystal and device physics, radiometric imaging; millimeter-wave and microwave technology.

Information Sciences Research Office: Program verification, program translation, performance-sensitive system design, distributed architectures for spaceborne computers, fault-tolerant computer systems, artificial intelligence, and microelectronics applications.

Materials Sciences Laboratory: Development of new materials: metal matrix composites, polymers, and new forms of carbon; component failure analysis and reliability; fracture mechanics and stress corrosion; evaluation of materials in space environment; materials performance in space transportation systems; analysis of systems vulnerability and survivability in enemy-induced environments.

Space Sciences Laboratory: Atmospheric and ionospheric physics, radiation from the atmosphere, density and composition of the upper atmosphere, aurorae and airglow; magnetospheric physics, cosmic rays, generation and propagation of plasma waves in the magnetosphere; solar physics, infrared astronomy; the effects of nuclear explosions, magnetic storms, and solar activity on the earth's atmosphere, ionosphere, and magnetosphere; the effects of optical, electromagnetic, and particulate radiations in space on space systems.